35th Annual International Conference of the IEEE EMBS
Osaka, Japan, 3 - 7 July, 2013

Multi-Stage Intra-Patient Template Matching for Prostate Detection in MR Volumes

Zeinab Jahed
University of California Berkeley
Bioengineering
Berkeley, United States
zjahed@berkeley.edu

Khaled Shaban
Qatar University
Computer Science and Engineering
Doha, Qatar
khaled.shaban@qu.edu.qa

Hamid R. Tizhoosh
University of Waterloo
Systems Design Engineering
Waterloo, Canada
tizhoosh@uwaterloo.ca

***Abstract*—Detecting objects, a significant task in computer vision, is accompanied with many challenges. When we focus on medical images, the challenges of detecting an organ or a tumour exhibit their own specific difficulties. Automatic finding of the prostate gland in magnetic resonance (MR) images, for instance, is a needed task in some clinical procedures. In this paper we propose a novel method for detection of the prostate gland in MR images. We use a multi-stage intra-patient approach to the template matching which is based on a trained dataset. We conduct experiments with the images of 100 patients and report preliminary results that seem to be promising.**

I. Introduction

Prostate cancer remains the most common type of cancer among men in the United States with nearly 30,000 deaths recorded annually [1]. Early detection and treatment of prostate cancer can significantly reduce the mortality rate of patients [1]. The detection process involves prostate localization followed by (mostly manual) segmentation, which is a labour-intensive task and requires skilled users. Therefore, full automation of the prostate gland localization and segmentation can considerably accelerate the prostate cancer detection process. A substantial amount of work has been dedicated to the automation of prostate segmentation [2]–[6]. However, most of these methods still require manual user inputs. For example, Vikal et al. propose a semi-automated method that requires user clicks on the prostate center in the central slice of the prostate volume to initiate segmentation [7]. Other methods require the user to manually identify reference points to mark the prostate gland as the region of interest [3]. In this paper, we present an unsupervised prostate region localization method, followed by automatic prostate detection. The MR volume data of a patient consists of several slices, including the full prostate volume from apex through mid-gland, to the base as shown in Fig. 1. This data set also includes the unwanted slices before the apex and after the base, which contain no portion of the prostate gland and hence are not required in subsequent segmentation steps. The objective of this work is first to eliminate the unwanted (irrelevant) slices, and second, to locate the prostate in each slice and crop the image to only contain the prostate gland. These two steps are required for any fully automated prostate segmentation and are especially difficult due to the variety of size, shape and positions of the prostate in MR images of different patients. Also, within the same MRI dataset of a given patient, the slices directly before and after the apex and base slices, respectively, are hardly distinguishable even for many skilled clinicians (Fig. 2).

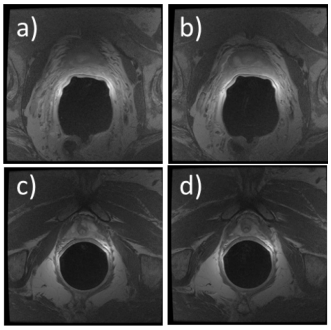

Fig. 2: (a) Slice with no prostate portion, (b) apex, (c) base, (d) slice with no prostate portion after the base.

In this paper, we introduce a multi-stage and intra-patient method, which uses the mid-gland slice (the slice with the largest cross-section of the prostate) to localize the prostate gland in all other slices, and thus to eliminate the unwanted (irrelevant) images.

II. Multi-Stage and Intra-Patient Template Matching for Prostate Detection

The proposed method consists of prostate region localization, and prostate detection as described below.

A. First Stage: Prostate region localization

The proposed method consists of a first stage to automatically localize the prostate region, followed by a second stage for intra-patient prostate detection. The goal of the first stage is to automatically locate the prostate region, and to find a slice within the patient's MRI volume data that contains a portion of the prostate gland. This goal was achieved by using a normalized square difference (NSQDIFF) template matching technique. In this method, all slices within a MRI dataset (of one patient) were used as source images and compared to a database of mid-gland prostate templates using

978-1-4577-0216-7/13/$26.00 ©2013 Crown

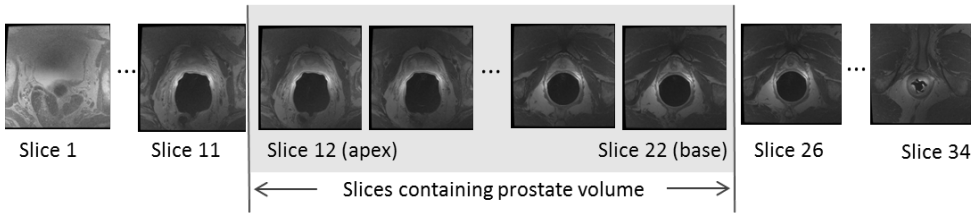

Fig. 1: Sample MR image data with 34 slices, where only slices 12–22 contain portions of the prostate volume.

$$R(x,y) = \frac{\sum_{x',y'}(T(x',y') - I(x+x',y+y'))^2}{\sqrt{\sum_{x',y'} T(x',y')^2 \times \sum_{x',y'} I(x+x',y+y')^2}} \quad (1)$$

where R is evaluated at each point (x, y) as the template image (T) slides over each MR source image (I) in one-pixel steps [8]. The highest matching probability in each MR source image is the location (x, y) with a minimum value of R. An overall minimum value of R is also updated as the program iterates through all the patients' MR volume slices to find the slice most similar to a mid-gland slice. Finally, the slice with the highest match, (i.e. lowest normalized square difference value R), is cropped to the size of the best-matched template. The best-matched slice and its location are used in the subsequent stage as a basis for intra-patient prostate detection. A schematic view of the first stage of this method is shown in Fig. 3. Algorithm 1 summarizes the first stage.

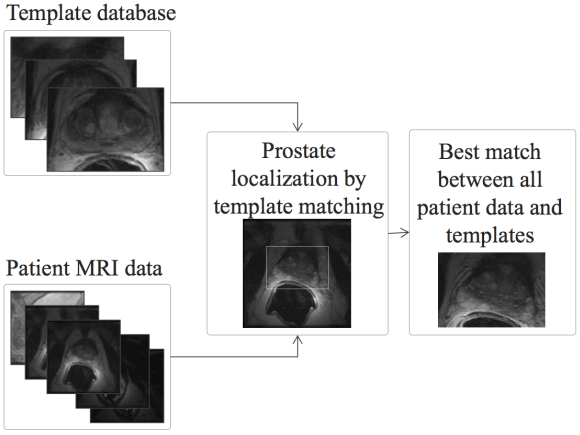

Fig. 3: Prostate region localization and identification.

Algorithm 1 Stage 1: Prostate Localization

```
for all images in template database do
  for all slices in patient's MRI volume data do
    MRslice ← read one MR slice
    Template ← read template image
    locate prostate region in MRslice through matching
    similarity ← normalized squared difference of template and located prostate region in MRslice
    if similarity > overall dissimilarity then
      overallsimilarity ← similarity
      bestmatchregion ← prostateregion
      bestmatchslice ← MRimage
    end if
  end for
end for
```

B. Second Stage: Prostate detection

The next stage involves the detection of prostate gland slices and the elimination of unwanted MR images. Initially, the best match slice found in the previous stage was compared to the same region on all other images in the patient's prostate volume data as depicted in Fig. 4. The second stage is given in Algorithm 2. Three different similarity/dissimilarity measures were used including normalized square difference (NSQDIFF), normalized cross correlation (NCCORR), and normalized correlation coefficient (NCCOEFF) (dissimilarity, measured by NSQDIFF, was inverted to a similarity measure before inputing into Algorithm 2). Using the same measures, all slices preceding the best-matched slice, and all slices after the best-matched slice were compared with the patient's first and last slices, respectively. The obtained similarity/dissimilarity values for the patient shown in Fig. 1 using this method are plotted in Fig. 5, where the horizontal axis represents the slice number and the vertical axis represents the similarity/dissimilarity values using NSQDIFF, NCCORR, and NCCOEFF. It is evident from the plots that in all three methods, the similarities increase for slices closest to the best-matched with a peak at the best match slice (perfect match), and decrease towards the first and last slices. However, due to strong variability detection based on a pre-set threshold was not successful. To overcome this problem, all images preceding the best match slice were compared with the patient's first slice and all images following the best match slice were compared to the last slice. Images with a lower dissimilarity (or higher similairty) to the first or last slice were marked as unwanted images. The detected region of slices containing the prostate volume, using the three different dissimilarity measures is shown as a shaded gray area in Fig. 5. Ideally, the first and last slices in this region are the apex and base, respectively. Different results were obtained from the three different similarity/dissimilarity measures. For this particular patient (Fig. 1), slices 12 and 22 are identified as the apex and base by an expert. The squared difference and correlation coefficient methods are sensitive, i.e. detect all slices containing the

prostate accurately, however, some unwanted images are not correctly identified. The cross correlation method on the other hand has a higher overall accuracy but leaves out slices containing the prostate volume. From an application point of view, elimination of slices containing a portion of the prostate volume is highly undesirable, i.e. the method must have a very high sensitivity. Therefore a combination of these methods was also evaluated.

Algorithm 2 Stage 2: Prostate Detection

for all slices in patient's MRI volume data **do**
  $first\ slice \leftarrow best\ match\ region$ on first slice
  $last\ slice \leftarrow best\ match\ region$ on last slice
  $match\ slice \leftarrow best\ match\ region$ on $best\ match\ slice$
  for all slices before $matchslice$ **do**
    $similarity1 \leftarrow$ compare with $First\ slice$
    $similarity2 \leftarrow$ compare with $match\ slice$
  end for
  for all slices after $matchslice$ **do**
    $similarity1 \leftarrow$ compare with $Last\ slice$
    $similarity2 \leftarrow$ compare with $match\ slice$
  end for
  if $similarity1 > similarity2$ **then**
    current slice contains the prostate
  else
    current slice does not contain the prostate
  end if
end for

III. Experiments, Results and Discussions

In this section, we provide information about the image data set we used for experiments, establish quantitative measures for performance assessment, and report experimental results.

A. Image Data

In order to conduct experiments, we used MR images collected from an online archive database (The online database is available at "*prostateMRimageDatabase.com*"). The images consist of T2-weighted magnetic resonance images (T2W) with endorectal coil. The volume set has a slice thicknesses ranging from 2.5 mm to 4.0 mm. The contrast of different image sets vary greatly as they have been captured with different machines and different configurations. The image sizes range from 256×256 up to 512×512 pixels. The total number of individual slices that contain a portion of prostate (based on manual delineation by one expert) is about 1100 images from a total of 3310 images for 100 patients.

B. Performance Measurement

We measure and report the following quantities:

- P_{mid}: Total number of cases with identified midgland
- N_P: Total number of images accurately detected as containing prostate

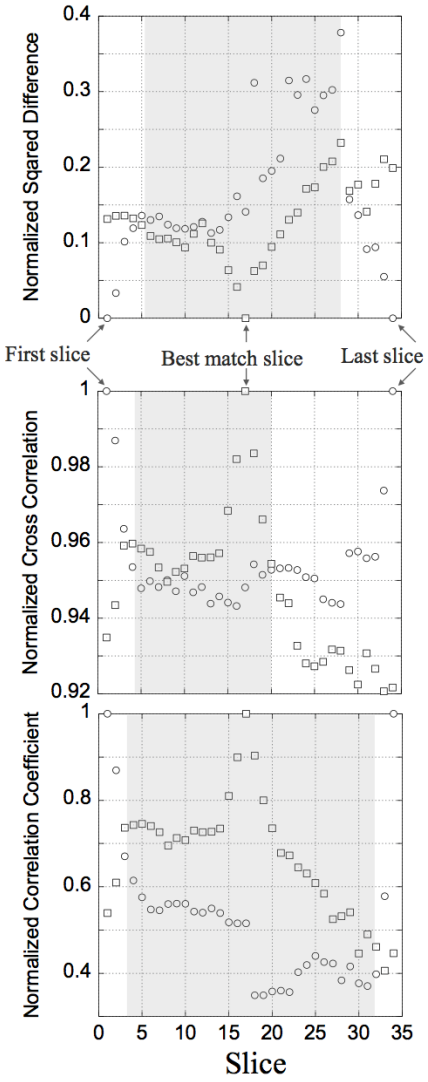

Fig. 5: Plot of similarities of MR volume of one patient, compared to the best-matched slice, first slice and last slice using (a) normalized square difference (b) normalized cross correlation, and (c) normalized correlation coefficient.

- SEN: Percentage of images accurately detected as containing prostate (Sensitivity)
- N_{ACC}: Total number of images accurately detected as with or without prostate (Accuracy)
- ACC: Percentage of images accurately detected as with or without prostate (accuracy)

C. Results

The template database for the prostate region localization step contains several size variations of the mid-gland prostate slice of a single patient. The average results for 5 different template databases are summarized in Table I (randomly selected patients used to create the database each time). In Table I, method A uses NSQDIFF, method B uses NSQDIFF and NCCOR or NSQDIFF and NCCOEFF, and method C uses NSQDIFF and NCCOR or NSQDIFF and NCCOEFF or NCCOEFF and NCCOR.

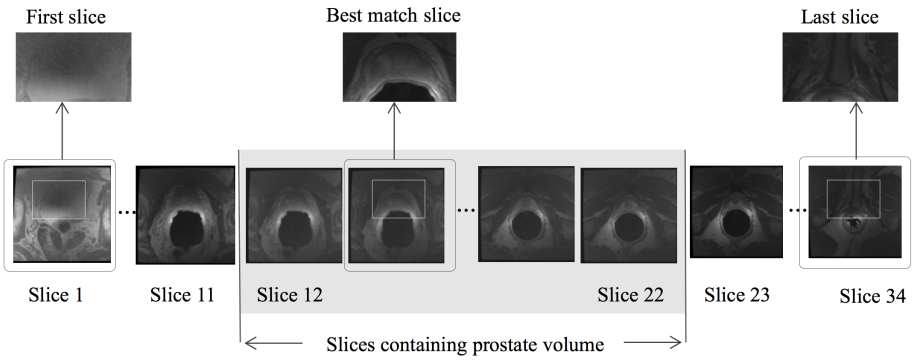

Fig. 4: Illustration of the first, best-matched, and last slices used to find all slices containing prostate.

Prostate region localization was very successful using this method with 0% false region detections. For 86% of the patients, the detected best-matched slice was correctly within the prostate volume slices.

TABLE I: Summary of average results obtained from 5 different prostate template databases.

	Method A	Method B	Method C
P_{mid}	85.66 ± 4.13	81.41 ± 4.72	84.44 ± 3.47
N_P	964 ± 37	927 ± 37	952 ± 30
SEN	87.36 ± 3.36	83.97 ± 3.34	86.27 ± 2.71
N_{ACC}	2094 ± 73	2181 ± 41	2185 ± 39
ACC	63.26 ± 2.20	65.90 ± 1.24	66.01 ± 1.17

The overall results summarized in Table I can be further increased by improvement in the detection of the prostate best match slice. Prostate detection was much more accurate in patients where the detected best match slice was closest to the prostate mid gland. This can be achieved by improving the prostate template database to contain more samples. For example, the database can contain average images of the mid-gland slices of several patients. It is important to note the difficulty, size and diversity of the image volume sets we have used for the experiments (see section III-A). All in all, this is a real-world and hence very challenging dataset. In spite diversity and low quality of images, the number of images is quite large compared to reported experiments in literature.

Other common object detection methods such as Viola-Jones and cascade classifier training, with local binary-feature-based classifiers were also tested for this work. However, the Viola-Jones method delivered high false detection rates. Local binary patterns can also be used to detect an object based on texture extraction/encoding but were not well suited for our application. Our experiments showed low detection accuracies in range of mid 60%. The fastest and most accurate results were obtained from the classic template matching method.

IV. Conclusions

Automatic localization and detection of prostate gland is required for any fully automated prostate segmentation software. A novel multi-stage intra-patient method was presented for prostate detection in MR volume data. The presented method is multi-stage consisting of an initial prostate localization stage followed by prostate detection. Intra-patient slice information was utilized to detect the prostate in all other slices of the same patient. Template matching was used in each stage with three different dissimilarity measures and 5 random variations of the template database. Our method was tested on MR volume data of 100 patients, consisting of a total of 3310 MR images. Results for stage one showed 86% successful localization of the prostate region followed by 87% sensitivity in stage two. An accuracy of 66% was achieved in stage 2 which can be improved significantly by an improved prostate mid-gland localization in stage one.

Acknowledgments – This work was funded by a Qatar University Internal Grant (QUUG-ENG-CSE-11/12-21) and a NSERC Discovery Grant (Canada). The authors also thank Segasist Technologies for providing DICOM images.

References

[1] A. Jemal, R. Siegel, J. Xu, and E. Ward, *Cancer Statistics*, 2010 BOTH SEXES FEMALE BOTH SEXES ESTIMATED DEATHS, vol. 60, no. 5, pp. 277–300, 2010.

[2] S. Martin, V. Daanen, and J. Troccaz, *Atlas-based prostate segmentation using an hybrid registration*, International Journal of Computer Assisted Radiology and Surgery, vol. 3, no. 6, pp. 485–492, 2008.

[3] D. Flores-Tapia, G. Thomas, N. Venugopal, B. McCurdy, and S. Pistorius, *Semi automatic MRI prostate segmentation based on wavelet multiscale products*, Annual International Conference of the IEEE Engineering in Medicine and Biology Society, vol. 2008, pp. 3020–3, 2008.

[4] D. Pasquier, T. Lacornerie, M. Vermandel, J. Rousseau, E. Lartigau, and N. Betrouni, *Automatic segmentation of pelvic structures from magnetic resonance images for prostate cancer radiotherapy*, International journal of radiation oncology, biology, physics, vol. 68, no. 2, pp. 592–600, 2007.

[5] S. Ghose, A. Oliver, R. Marti, X. Llad, J. Freixenet, J. C. Vilanova, F. Meriaudeau, D. Bourgogne, L. Cnrs, and L. Creusot, *A probabilistic framework for automatic prostate segmentation with a statistical model of shape and appearance*, University of Girona , Computer Vision and Robotics Group , Girona , Spain . Girona Magnetic Resonance Center , Girona , Spain ., pp. 713–716, 2011.

[6] S. Klein, U. a. van der Heide, I. M. Lips, M. van Vulpen, M. Staring, and J. P. W. Pluim, *Automatic segmentation of the prostate in 3D MR images by atlas matching using localized mutual information*, Medical Physics, vol. 35, no. 4, p. 1407, 2008.

[7] G. F. Vikal, S., S. Haker, C. M. Tempany, *Prostate contouring in MRI guided biopsy*, in NIH Public Access, 2010.

[8] Open Source Computer Vision Library Reference Manual, Intel Corporation, 2001